JOURNAL OF BONE AND MINERAL RESEARCH
Volume 15, Number 4, 2000

Chromosomal Mapping of Osteopenia-Associated Quantitative Trait Loci Using Closely Related Mouse Strains

HELEN BENEŠ,[1] ROBERT S. WEINSTEIN,[3–5] WENHUI ZHENG,[1] JOHN J. THADEN,[2,3] ROBERT L. JILKA,[3–5] STAVROS C. MANOLAGAS,[3–5] and ROBERT J. SHMOOKLER REIS[1–3,5]

ABSTRACT

Peak bone mineral density (BMD) is a highly heritable trait in humans and is currently the best predictor of skeletal fragility underlying osteoporosis. The SAMP6 mouse strain displays unusually low BMD at maturity, and age-dependent osteopenia associated with defective osteoblastogenesis. To identify quantitative trait loci (QTLs) influencing bone density, we constructed crosses between SAMP6 and either AKR/J or SAMP6, two related mouse strains of higher peak BMD. Due to common ancestry of these strains, intercross parents differed at only 39–40% of 227 highly-polymorphic genotyping markers, thus restricting our search to this informative portion of the genome and reducing the number of mice required for QTL significance. Using dual energy X-ray absorptiometry (DEXA), we measured spinal BMD in F_2 cross progeny at 4 months of age, and selectively genotyped those in the highest and lowest quartiles for BMD. Based on linear regression of bone density on genotype, including Composite Interval Mapping to enhance mapping precision while adjusting for effects of distal markers, we identified multiple QTLs significantly affecting spinal BMD; these were mapped to regions of chromosomes 2 (two sites, one confirmed in both crosses), 7, 11, 13 and 16. One of these loci had been previously identified as a significant bone-density QTL, while 3 substantiate QTLs suggested by a low-power study of 24 recombinant-inbred mouse lines. Such recurrent appearance of QTLs, especially in crosses involving distantly-related strains, implies that polymorphism at these loci may be favored by evolution and might underlie variation in peak bone density among humans. (J Bone Miner Res 2000;15: 626–633)

Key words: **osteopenia, bone density, bone mineral density, quantitative trait loci, mouse, inbred strains, chromosomal mapping, genetic map**

INTRODUCTION

ONE OF the most important indicators of bone fragility in age-onset osteoporosis is bone mineral density (BMD), and a principle determinant of bone density in humans is heredity.[1] Based on the higher BMD correlation between monozygotic twins than between dizygotic twins and other familial studies of bone density, the heritability of bone density has been estimated at 60–70%.[2–6] Markers of bone turnover are more concordant in identical twins than dizy-

[1]Department of Biochemistry and Molecular Biology, University of Arkansas for Medical Sciences, Little Rock, Arkansas, U.S.A.
[2]Department of Geriatrics, University of Arkansas for Medical Sciences, Little Rock, Arkansas, U.S.A.
[3]Department of Medicine, University of Arkansas for Medical Sciences, Little Rock, Arkansas, U.S.A.
[4]Division of Endocrinology and Center for Osteoporosis and Metabolic Diseases, University of Arkansas for Medical Sciences, Little Rock, Arkansas, U.S.A.
[5]Central Arkansas Veterans Health Care System, Research-151, Little Rock, Arkansas, U.S.A.

gotic twins, implying that genetic factors also govern bone turnover rate.[6,7] Nevertheless, very little is known about the genetic regulation of BMD and bone turnover.

Mice provide a faithful model of human bone changes leading to osteoporosis. They exhibit similar cellular, biochemical, molecular, and histological changes after loss of gonadal function or with glucocorticoid excess.[8–12] Specific mouse strains undergo progressive osteopenia after maturity[13,14] accompanied by reduced number and function of osteoblasts,[11,12] similar if not identical to senescent bone changes in humans.[15] Inbred mouse strains differ in peak bone mass, bone turnover, age-related fracture, and response to physical activity.[16]

SAM strains were derived from an AKR/J stock by Takeda and coworkers and maintained by brother-sister mating for over 80 generations.[17] The SAMP lines, described as having accelerated senescence, originated from litters with exceptional traits of reduced fitness coupled with marked reduction or absence of thymic leukemias, which are characteristic of the AKR/J parental strain. Osteopenia was observed in lines SAMP6 and SAMR3 (and to a lesser extent in SAMP9) but not in other SAM lines, based on microdensitometry of soft X-ray images of the femoral diaphysis in young adult mice.[17,18] These histomorphometric analyses indicated a reduction in bone mass for the osteopenic lines, relative to other SAM lines. Our own recent data using quantitative dual-energy X-ray absorptiometry (DEXA) scanning have confirmed the deficit in peak bone mass for SAMP6 mice at 4 months of age and have suggested a marked age-dependent decline in BMD after maturity.[19] We also showed reduced bone formation rate, defective osteoblastogenesis, and increased adipogenesis and myelopoiesis in SAMP6 mice relative to higher bone-density strains SAMR1[20–22] and AKR/J (Weinstein R. S., Jilka R. L., and Manolagas S. C., unpublished data), probably involving altered expression of PPARγ2 or its ligand(s).[22]

In the present study, we have sought genetic differences underlying interstrain variation in peak BMD, through the use of powerful analytic tools available for the detection of quantitative trait loci (QTLs). We employed DEXA to obtain rapid and reproducible measurements of spine BMD,[19] and selective genotyping followed by single-marker and interval-mapping analyses, to identify chromosomal regions strongly associated with peak bone density. We report evidence from two interstrain crosses, for five to six highly significant bone-density QTLs, of which only one had previously been detected with statistical significance.

MATERIALS AND METHODS

Animals and construction of interstrain crosses

SAMP6 and SAMR1 mice were obtained from a colony established using breeders kindly provided to us by Dr. Toshio Takeda of Kyoto University (Kyoto, Japan).[17,18] AKR/J mice were obtained from The Jackson Laboratory (Bar Harbor). All mice were maintained under standard laboratory conditions (12:12 light/dark cycle, 20°C, and 48% humidity) and treated in accordance with U.S. National Institutes of Health guidelines on care and use of laboratory animals. Mice received a standard diet (Agway RMH-3000, Harlan Teklad, Madison, WI, U.S.A.) with water ad libitum. Individual animals were electronically tagged (Biomedic Data Systems, Inc., Seaford, DE, U.S.A.) at weaning and housed with sexes segregated. Strains were maintained by brother-sister mating, preserving lineage diversity. Crosses were constructed by reciprocal matings between SAMP6 mice and either the SAMR1 or the AKR/J strain, with two females and one male per cage.

Bone densitometry

DEXA was performed on a QDR-2000+ densitometer (Hologic, Inc., Bedford, MA, U.S.A.) as previously described.[19] Briefly, 250 F_2 mice were scanned at 118–134 (mean 126) days of age, in the prone position with tape attached to each spread limb on a precision-milled acrylic block. Spinal BMD was scanned from below the skull to the base of the tail. Accuracy of DEXA measurements was indicated by high reproducibility ($\sim$2% coefficient of variation) and a strong correlation ($r > 0.95$) between BMD and ash weight.[19]

Genotyping

Genomic DNA was isolated from 2.5-cm tail snips of individual mice (Puregene, Gentra Systems, Minneapolis, MN, U.S.A.). For assessment of specific microsatellite markers, polymerase chain reaction (PCR) amplification was performed using a Deltacycler (Ericomp, Inc., San Diego, CA, U.S.A.) and site-specific flanking primers (Research Genetics, Huntsville, AL, U.S.A.), modifying the standard annealing temperature as required to improve specificity. PCR products were visualized by autoradiography or phosphorimager analysis (Molecular Dynamics, Sunnyvale, CA, U.S.A.) after electrophoresis through nondenaturing 8% polyacrylamide gels.

Data analysis

Differences in BMD among the three mouse strains were evaluated for significance by Fisher's *t*-test.[23] Broad-sense heritability (H^2) is defined as the fraction of total variance for a trait, which is attributable to genetic variance. It was calculated as $[V_{F2} - V_{F1}]/V_{F2}$, or $[V_{F2} - V_P]/V_{F2}$, where V_{F2}, V_{F1}, and V_P refer to the variance (s^2) of the F_2, F_1, and parental generations, respectively. Linkage maps were determined from actual F_2 genotypes using Mapmaker.[24] The resultant maps were input to QTL Cartographer,[25] which was used to perform univariate linear regression, stepwise multivariate regression, and Composite Interval Mapping (CIM),[26] as well as permutation of phenotypes with respect to genotypes to estimate false-positive thresholds[27,28] for both linear regression and CIM. Interval mapping of putative QTLs utilized the CIM procedure of Zeng[26] as implemented in the QTL Cartographer software package (v. 1.13).[25] CIM analyses used a window size of 15, and 4–6 background variables ranked by stepwise regression, requir-

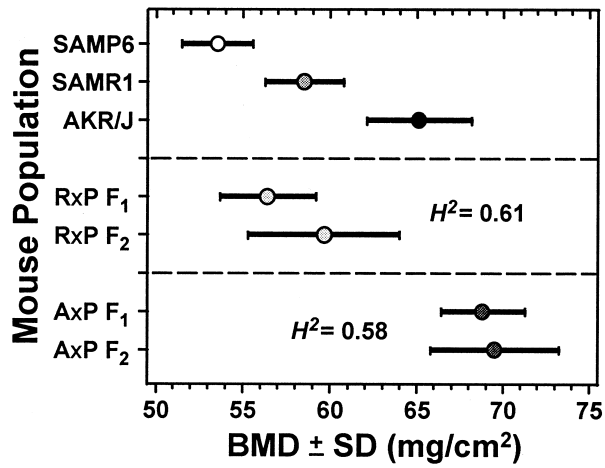

FIG. 1. Analysis of BMD in related mouse strains. Mice of strains AKR/J, SAMR1, and SAMP6, each at 118–134 days of age, were scanned by DEXA using a Hologic 2000+ densitometer to quantitate BMD (in mg/cm^2 ± SD) as described in the Methods section. Data for the two sexes were combined, no differences in peak BMD having been observed between males and females of these three strains or their cross progeny. Pairwise differences among strains were evaluated by Fisher's *t*-test, with the following false-positive values: $P < 0.005$ between SAMP6 and SAMR1 and $P < 0.001$ between SAMP6 and AKR/J. BMDs also are shown for F_1 and F_2 mice derived from SAMR1 × SAMP6 and AKR/J × SAMP6 crosses. Broad-sense heritability (H^2) values shown were calculated from the greater variance of segregating F_2 mice than from genetically homogeneous F_1 mice,[31] as described in the Materials and Methods section.

ing $F > 9$ for marker inclusion. Very similar results, typically with broader peaks, also were obtained by the interval mapping procedure of Lander and Botstein[29] (data not shown).

RESULTS

DEXA, modified for application to small mammals, allowed highly reproducible measurement of BMD (in mg/cm^2) on live mice.[19] This procedure provides a measure of bone density, which is representative of the entire skeleton or subregion thereof. In the present studies, we have focused on spinal BMD, because of its relatively low within-group variance. At 4 months of age, mature SAMP6 mice exhibit a spinal BMD 9% lower than SAMR1 ($P < 0.005$) and 18% lower than AKR/J ($P < 0.001$) (Fig. 1). The SAMP6 strain was crossed with AKR/J or SAMR1, in a reciprocal mating protocol, and the F_2 progeny were analyzed for BMD at 4 months of age. The increase in mean BMD, of F_1 and F_2 mice relative to their parents, implies inbreeding depression of bone density in parental strains, especially AKR/J. Broad-sense heritability (H^2) of bone density was calculated for each cross from the increased variance among F_2 mice, relative either to the parental strains (mean of variances) or to their F_1 progeny. Values derived from four such comparisons ranged from 0.53 to 0.76, averaging ~0.62, quite similar to estimates for the heritability of human BMD.[1–5]

We identified informative markers that distinguish among these strains, for genotyping the F_2 progeny of each cross. Genomic DNA fragments from the AKR/J, SAMR1, or SAMP6 strains were amplified using primer pairs flanking microsatellite markers characterized at the Whitehead Institute,[30] with a mean spacing of <7 map units (centi-Morgans [cM]). The three strains shared a common allele at 44% of markers, whereas any two strains differed at 39–40% of loci, primarily situated in clusters similar to the parental-origin blocks of recombinant-inbred lines.

F_2 mice in the highest and lowest 25% of BMD values were genotyped, because these contribute >90% of the mapping information to be derived from the cross.[29] Single-marker linear regressions against 4-month BMD were performed at informative markers, the most significant of which are shown in Tables 1 and 2. Significance thresholds were determined both analytically from the regression *F* statistics (columns labeled P_F), and empirically (generating false-positive frequencies P_e) by conducting 10,000 permutations of phenotypes with respect to genotypes, each followed by reanalysis of all marker regressions.[27,28] Empirical thresholds were tallied from complete genome scans and thus do not require further (Bonferroni) correction for multiple determinations. Multivariate linear regression models were then derived by a heuristic stepwise-regression algorithm of marker addition and elimination.[25] The strongest associations detected in the AKR/J × SAMP6 cross were on chromosomes 2 and 11 (Table 1), each achieving significance at a genomewide $P_e \leq 0.001$ for two peak markers; a weaker but significant peak ($P_e \leq 0.025$) also was seen on chromosome 13. Analysis of the SAMR1 × SAMP6 cross revealed additional QTLs on chromosomes 7 (genomewide $P_e < 0.002$) and 16 ($P_e < 0.01$). No chromosome-2 markers were significant by univariate linear regression in this cross, but two were highly significant ($P \leq 0.001$; not shown) by multivariate regression (Table 2). The discrepancy may be caused by allelic interactions with other loci, also suggested by diallele analysis indicating non-independent (interactive) effects between loci near *D2Mit296* and *D7Mit227* ($P \leq 0.01$ by Fisher's exact test) and perhaps between *D2Mit296* and *D15Mit11* ($P \leq 0.025$).

Single-marker regressions indicating the effects of genotype on BMD are shown in Figs. 2A–2C for markers on chromosomes 2, 7, and 11 exhibiting the highest significance of association. These loci have primarily an additive effect, with relatively little dominance. For example, regression at the chromosome-2 peak (Fig. 2A) showed an additive effect *a* of 2.8 mg/cm^2 per AKR or SAMR1 allele, and a dominance *d* (deviation from additivity in the heterozygote) of 0.3 mg/cm^2. Although the AKR and SAMR1 alleles at the loci on chromosomes 2 and 16 confer higher bone density than the SAMP6 allele, on chromosomes 7, 11, and 13 it is the SAMP6 alleles that favor higher BMD (Figs. 2B and 2C). Countervailing allelic effects in parental strains produce "transgressive segregation" (F_2 phenotypes more extreme than parents),[31] evident in Fig. 1. The differences

TABLE 1. AKR/J × SAMP6 F_2 ANALYSIS: SINGLE-MARKER STATISTICS

Locus	*Map position (cM)*	*Univar. linear regression* F	P_F	*Permutation* P_e (*genomewide* α)	*Multivariate regression* F
D2Mit312	2.2	9.4	0.003	~0.05	—
D2Mit119	7.7	18.7	<0.0001	<0.001	11.3
D2Mit464	10.9	19.5	<0.0001	<0.001	23.6
D2Mit296	23	15.6	<0.0001	<0.005	—
D11Mit284	49	23.1	<0.0001	<0.001	25.2
D11Mit160	60	17.7	<0.0001	<0.001	—
D13Mit20	22	10.7	0.001	<0.025	—

TABLE 2. SAMR1 × SAMP6 F_2 ANALYSIS: SINGLE-MARKER STATISTICS

Locus	*Map position (cM)*	*Univar. linear regression* F	P_F	*Permutation* P_e (*genomewide* α)	*Multivariate regression* F
D2Mit312	2.2	—	—	—	13.0
D2Mit296	23	—	—	—	19.2
D7Mit210	11	16.6	<0.001	<0.002	—
D7Mit227	13	12.4	0.001	<0.01	15.0
D16Mit100	9	5.7	0.02	0.02	—
D16Mit39	28.4	10.7	0.001	<0.01	13.7

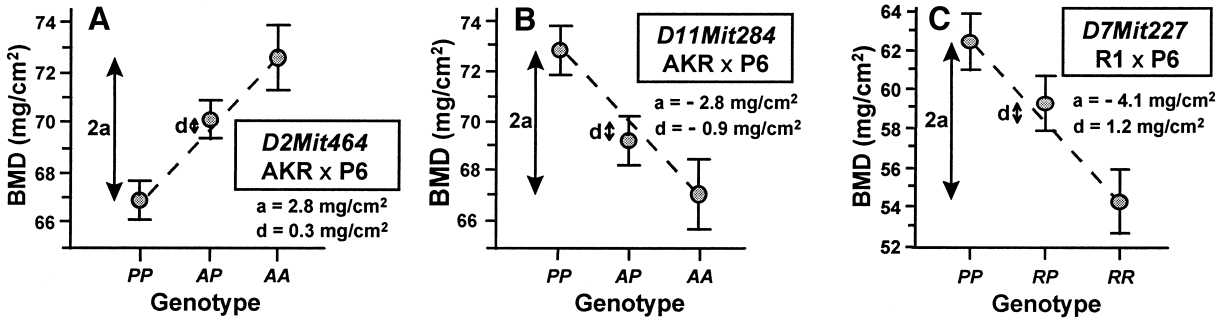

FIG. 2. Regressions of phenotype on genotype, analyzed for F_2 mice from two independent crosses. The effects of genotype on spinal BMD (based on genotype data for F_2 mice in the upper and lower 25% of spinal BMD) were plotted for markers showing significant *F* statistics from single-marker analysis of the two crosses (Tables 1 and 2). (A and B) Regressions at markers (*D2Mit464* and *D11Mit284*, respectively) segregating in an AKR × SAMP6 cross. (C) Regression at marker *D7Mit227*, segregating in a SAMR1 × SAMP6 cross. Genotypes: *P* represents the SAMP6 allele at the indicated locus, *R* the SAMR1 allele, and *A* the AKR/J allele. Note that SDs are exaggerated by the selective genotyping of phenotypic extremes.

between parental strains at 4 months of age (Fig. 1) are not predictable from the significant BMD loci detected thus far, implying that additional QTLs of smaller effect remain to be discovered.

Composite Interval Mapping (CIM) was conducted within QTL Cartographer, using background markers prioritized by stepwise multivariate regression for each cross.[25,26] CIM combines interval mapping, in which likelihood ratios are calculated incrementally between markers,[29] with multiple linear regression, which includes effects of remote marker genotypes when evaluating each interval.[26] All interval mapping procedures, including CIM, lose some power relative to single-marker analysis for significance at each marker but provide superior positional information.[31]

A broad QTL peak was localized on chromosome 2 (Fig. 3A) near the centromeric end (left of each map), based on analysis of AKR/J × SAMP6 F_2 progeny. The peak likelihood ratio (LOD of 4.05) exceeded the $\alpha = 0.01$ threshold for false positives occurring anywhere in the genome (dashed lines, Fig. 3), which was determined empirically from 1000 trait permutations.[27,28] Similar analysis of SAMR1 × SAMP6 F_2 mice localized a much sharper peak, with a 1-LOD (>95% confidence) interval[31] 11 cM in width, positioned slightly farther from the centromere (Fig. 3B). Although the peaks appear non-coincident, marker regression analyses indicated high significance at *D2Mit296* in both crosses (Tables 1 and 2). These combined data implicate the presence of two neighboring QTLs in the AKR/J × SAMP6 cross, producing a broad peak on chro-

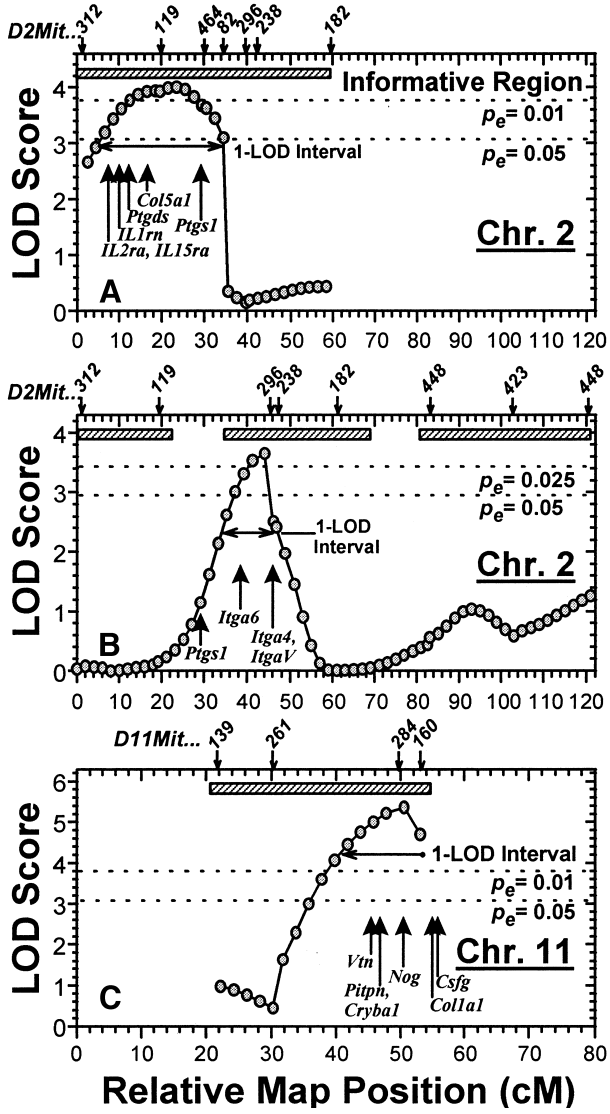

FIG. 3. CIM of bone-density QTLs on chromosomes 2 and 11. (A) Map of chromosome 2, based on analysis of an AKR × SAMP6 cross. (B) Map of chromosome 2, derived from a SAMR1 × SAMP6 cross. (C) Map of chromosome 11, derived from an AKR × SAMP6 cross. Genotypes were determined for F_2 mice in the upper and lower quartiles of BMD distribution for each cross, at the indicated markers. Likelihood ratios were determined by CIM,[26] as implemented by QTL Cartographer,[25] and converted to LOD scores (LOD = Likelihood Ratio/4.6). Marker positions (with names abbreviated, e.g., *312* for marker *D2Mit312*) are indicated by arrows above each panel. For reference, several candidate genes mapped near each peak are indicated below the curves, with arrows pointing upward. Hatched boxes mark informative regions, within which the parental strains could be distinguished. A horizontal double arrow indicates the 1-LOD support interval for each QTL, corresponding in theory to a 96% confidence interval for peak position.[31] Empirical significance thresholds (false-positive levels of 0.01, 0.025, or 0.05 on a genomewide scan), shown as dashed horizontal lines, were determined by 1000 random permutations of phenotypes with respect to genotypes.[27,28]

mosome 2 (Fig. 3A). Such "ghost" peaks often appear between nearby QTLs, by summation of effects not resolvable over short linkage intervals.[31] In each cross, the QTL peak on chromosome 2 was estimated to confer an additive effect of 2.4–2.8 mg/cm^2 with little dominance (data not shown), consistent with single-marker analyses (Fig. 2A). CIM indicated a sharp maximum-likelihood peak on chromosome 7, exclusively in the SAMR1 × SAMP6 cross, between the *D7Mit210* and the *D7Mit227* markers implicated in single-marker analysis. Although these marker-BMD associations were highly significant by regression at individual markers (Table 2), the interval mapping peak did not reach genomewide significance at the 0.05 level (data not shown). On chromosome 11, interval mapping of the AKR/J × SAMP6 cross achieved a maximal LOD score of 5.4 (genomewide $P_e \ll 0.01$), near marker *D11Mit284* (Fig. 3C).

None of the above results were altered substantially by inclusion of mouse weight, age (118–134 days), or sex in the regression models, consistent with data (not shown) indicating that all parental strains were similar in weight at maturity, were close to peak BMD at 4 months of age, and did not differ by sex in bone density. Moreover, when mouse weight was considered as the primary trait, no significant QTLs were detected (by linear regression, stepwise regression, or composite interval mapping) and no QTL peaks of any magnitude appeared at the positions or markers where BMD likelihood peaks were situated.

DISCUSSION

Interstrain crosses were performed between SAMP6, a low-BMD mouse strain, and two related strains (SAMR1 and AKR/J, each identical to SAMP6 at ~60% of polymorphic markers), which display bone densities 9% and 18% higher than SAMP6, respectively. Through single-marker analysis and CIM (multivariate interval mapping), we have identified QTLs that strongly affect BMD in the three mouse strains studied; each produced an additive effect on BMD within the range of 2–4 g/cm^2 per allele. Significance of these loci was determined empirically, by random permutation of the observed F_2 phenotypes with respect to genotypes, and was in each case evaluated for false-positive occurrences across the entire genome. At least five statistically significant loci were detected, situated on chromosomes 2, 7, 11, 13, and 16. Of these loci, only those on chromosomes 2 and 16 help to "explain" the low spinal BMD of strain SAMP6, in that the allele found in this strain confers lower bone density than the allele of the other parental strain. The observation of countervailing alleles (e.g., Figs. 2B and 2C) is quite common in QTL studies and indeed accounts for the segregation of F_2 mice with phenotypes more extreme than either parent (see Fig. 1). We infer that many further spinal-BMD QTLs of lesser effect have yet to be discovered, so that the sum of all QTL effects—if all were known—would be consistent with the bone densities of the parental strains.

On chromosome 2, the maximum-likelihood peaks generated in the two crosses fall in the same vicinity—the "top"

(centromeric) 50 cM of this chromosome—but they are not identical (compare Fig. 3A with 3B). Together, they confirm the presence of one or more QTLs affecting bone density in this region. However, the breadth and relative flatness of this peak in the AKR × SAMP6 cross (Fig. 3A) are indicative of two or more nearby loci, which cannot be resolved by interval mapping because of the low probability of recombinations occurring between them in the F_2 data set, thus generating a spurious peak between the actual QTLs.[31] This interpretation is supported by the high significance of marker *D2Mit296* in both crosses by univariate regression analyses (Tables 1 and 2); unlike CIM, this procedure is unaffected by trait associations with neighboring markers. We therefore infer the presence of two loci with strong BMD effects in the AKR × SAMP6 cross, one near *D2Mit296* and the other lying closer to *D2Mit312*. (The latter locus would not have been detected in the SAMR1 × SAMP6 cross unless the underlying QTL also differed between those parental strains, so as to confer different effects on BMD.) Resolution of these two loci and confirmation of all QTLs detected will depend on the isolation of either allele for each locus in the contrasting genetic background, through backcrossing recursively to one of the parental strains. Flanking markers will be monitored during the course of this introgression, and late-arising recombinants will be analyzed in order to narrow the region of gene localization. These experiments are currently in progress.

BMD measurements might be expected to depend to some extent on body weight, because of load effects and the way in which BMD is assessed by DEXA, as a projection of a three-dimensional parameter (bone mineral content) on a two-dimensional plane. We began with mouse strains that differ little in mature body weight or skeletal dimensions, but this does not guarantee that QTLs governing those traits would not segregate in interstrain crosses. It is thus reassuring that no body-weight QTLs were detected and that there was no effect on the QTLs we mapped for BMD, upon inclusion of weight as an independent variable in the multivariate linear regressions used for genetic mapping.

Recently, two other published reports have addressed the genetic mapping of mouse loci affecting BMD. DEXA analysis of 3-month-old female mice from 24 BXD (C57BL/6 × DBA/2) recombinant-inbred lines implicated 10 possible QTLs.[32] Although this study lacked the power to assure accurate positioning or to attain genomewide significance for any QTL, the positions of three loci (chromosome 2, 23 cM; chromosome 11, 59 cM; and chromosome 16, 25 cM) are remarkably consistent with our mappings (see Tables 1 and 2 and Fig. 3). Additional QTLs on chromosomes 2 and 7 did not coincide with our interval mapping, perhaps because of the limited positional information afforded by 24 recombinant-inbred lines. A recent analysis of male SAMP6 × SAMP2 F_2 mice[33] found highly significant bone-density QTLs on chromosomes 11 and 13, the first of which coincides within a few centiMorgans with the chromosome-11 peak reported here. The second, on chromosome 13, lies 18–25 cM from our nearest informative marker, at which we also found significant association with BMD; thus it is possible that these QTLs also are coincident, but we will need additional informative markers in a predominantly allele-identical region to resolve this question. We also should note that a human locus (11q12–13) associated with high bone mass[34] corresponds to segments of mouse chromosomes 2, 7, and 19, of which only the syntenic region near *Ssrp1* (52.4 cM on murine chromosome 2) lies close to a QTL identified in the present study.

The recurrent identification of the same chromosomal regions in multiple crosses, between strains either closely[33] or distantly[32] related to those utilized here, is noteworthy because it implies that the underlying QTL polymorphisms must be widespread. Conservation of functional polymorphism among diverse strains—a prerequisite for genetic mapping—suggests evolutionary maintenance of that polymorphism in a species, either by increased fitness of heterozygotes or because distinct alleles are favored in different environments. Bone density might be expected to show environment-specific polymorphism if speed (associated with lower bone density and hence weight) and bone mass (contributing to both structural strength and calcium reserves) are advantageous under different circumstances. Such duality of selection, should it apply to humans as well, may favor allelic diversity at the same loci as those mapped in mice.

Over a dozen genes affecting bone homeostasis have been localized near the QTLs we have observed to date (e.g., see upward arrows in Fig. 3). The list of such genes includes loci encoding collagen-IA1 (*col1a1*), the cytokine interleukin-11 (*IL-11*), an IL-1 receptor antagonist (*IL1RN*), the BMP-2/4 antagonist noggin (*Nog*), the granulocyte/monocyte-colony–stimulating factor (*Csfg*), several integrins (*Itga6*, *Itgsv*, and *Itga4*), and two prostaglandin synthases (*Ptgs1* and *Ptgds*), as well as the pro-apoptotic protein bax. We hasten to point out that the confidence interval for each QTL encompasses hundreds of genes, the vast majority of which are unknown, so that any discussion of the functional implications of the few genes noted above is highly conjectural. Nevertheless, certain of these loci have particular relevance to SAMP6 osteopenia, of which the reader should be aware. Notably, the reciprocal relationship between decreased osteoblastogenesis and increased adipogenesis in the SAMP6 mouse[22] may be explained by a change, in early mesenchymal progenitors, in expression of the *PPARγ* gene encoding a transcription factor (peroxisome proliferator–activated receptor γ) known to be critical for adipocyte differentiation.[35] Similarly, the SAMP6 phenotype might be due in part to allelic variation in *Ptgds* (encoding prostaglandin D2 synthase), which could affect the production of prostaglandins D2 and J2, a ligand of PPARγ. We also observed a QTL on chromosome 7 (see Table 2, marker *D7Mit210*) near the locus for IL-11, a potent inhibitor of adipogenesis that exhibits reduced expression in SAMP6.[36] Finally, allelic differences within the *noggin* gene, encoding a potent bone morphogenetic protein (BMP) antagonist, could account for the decreased osteoblastogenesis characteristic of the SAMP6 strain[19,20] in view of evidence that the balance between noggin and BMP-2/4 may determine the tonic baseline control of the rate of osteoblastogenesis.[37]

ACKNOWLEDGMENTS

We thank Randall S. Shelton, Regina Dennis, Ping Kang, and Timothy McClure for expert technical assistance. This work was supported by National Institutes of Health grant P01-AG13918, and by a REAP grant award from the U.S. Dept. of Veterans Affairs.

REFERENCES

1. Pocock NA, Eisman JA, Hopper JL, Yeates MG, Sambrook PN, Ebert S 1987 Genetic determinants of bone mass in adults: A twin study. J Clin Invest **80:**706–710.
2. Slemenda CW, Christian JC, Williams CJ, Norton JA, Johnston CCJ 1991 Genetic determinants of bone mass in adult women: A reevaluation of the twin model and the potential importance of gene interaction on heritability estimates. J Bone Miner Res **6:**561–567.
3. Hopper JL, Green RM, Nowson CA, Young D, Sherwin AJ, Kaymakci B, Larkins RG, Wark JD 1998 Genetic, common environment, and individual specific components of variance for bone mineral density in 10- to 26-year-old females: A twin study. Am J Epidemiol **147:**17–29.
4. Hansen MA, Hassager C, Jensen SB, Christiansen C 1992 Is heritability a risk factor for postmenopausal osteoporosis? J Bone Miner Res **7:**1037–1043.
5. Gueguen R, Jouanny P, Guillemin F, Kuntz C, Pourel J, Siest G 1995 Segregation analysis and variance components analysis of bone mineral density in healthy families. J Bone Miner Res **10:**2017–2022.
6. Kanis JA, Melton LJ 3rd, Christiansen C, Johnston CC, Khaltaev NJ 1994 The diagnosis of osteoporosis. J Bone Miner Res **9:**1137–1141.
7. Kelly PJ, Morrison NA, Sambrook PN, Nguyen TV, Eisman JA 1995 Genetic influences on bone turnover, bone density and fracture. Eur J Endocrinol **133:**265–271.
8. Girasole G, Jilka RL, Passeri G, Boswell HS, Boder G, Williams DC, Manolagas SC 1992 17β-estradiol inhibits interleukin-6 production by murine bone marrow stromal cells and human osteoblasts in vitro: A potential mechanism for the anti-osteoporotic effects of estrogens. J Clin Invest **89:**883–891.
9. Jilka RL, Hangoc G, Girasole G, Passeri G, Williams D, Abrams J, Broxmeyer H, Manolagas SC 1992 Increased osteoclast development after estrogen loss: Mediation by interleukin-6. Science **257:**88–91.
10. Bellido T, Jilka RL, Boyce B, Girasole G, Broxmeyer H, Dalrymple SA, Murray R, Manolagas SC 1995 Regulation of interleukin-6, osteoclastogenesis and bone mass by androgens: the role of the androgen receptor. J Clin Invest **95:**2886–2895.
11. Manolagas SC, Jilka RL 1995 Bone marrow, cytokines, and bone remodeling: Emerging concepts for the pathophysiology of osteoporosis. N Engl J Med **332:**305–311.
12. Weinstein RS, Jilka RL, Parfitt AM, Manolagas SC 1998 Inhibition of osteoblastogenesis and promotion of apoptosis of osteoblasts and osteocytes by glucocorticoids: potential mechanisms of their deleterious effects on bone. J Clin Invest **102:**274–282.
13. Silberman M, Weiss A, Resnick AZ, Edam Y, Seydel N, Gershon D 1987 Age-related trend for osteopenia in femurs of female C57BL/6 mice. Comp Geront **1:**45–51.
14. Kobayashi Y, Goto S, Tanno T, Yamazaki M, Moriya H 1998 Regional variations in the progression of bone loss in two different mouse osteopenia models. Calcif Tissue Int **62:**426–436.
15. Parfitt AM 1992 The two-stage concept of bone loss revisited. Triangle **31:**99–110.
16. Rogers J, Mahaney MC, Beamer WG, Donahue LR, Rosen CJ 1997 Beyond one gene-one disease: Alternative strategies for deciphering genetic determinants of osteoporosis. Calcif Tissue Int **60:**225–228.
17. Takeda T, Hosokawa M, Higuchi K 1994 Senescence-accelerated mouse (SAM). A novel murine model of aging. In: Takeda T (ed.) The SAM Model of Senescence. Elsevier Science, Amsterdam, pp. 15–21.
18. Matsushita M, Tsuboyama T, Kasai R, Okumura H, Yamamuro T, Higuchi K, Kohno A, Yonezu T, Utani A, Umezawa M, Takeda T 1986 Age-related changes in bone mass in the senescence-accelerated mouse (SAM). SAM-R/3 and SAM-P/6 as new murine models for senile osteoporosis. Am J Pathol **125:**276–283.
19. Jilka RL. Weinstein RS. Takahashi K. Parfitt AM. Manolagas SC 1996 Linkage of decreased bone mass with impaired osteoblastogenesis in a murine model of accelerated senescence. J Clin Invest **97**:1732–1740.
20. Kajkenova O, Lecka-Czernik B, Gubrij I, Hauser SP, Takahashi K, Parfitt AM, Jilka RL, Manolagas SC, Lipschitz DA 1997 Increased adipogenesis and myelopoiesis in the bone marrow of SAMP6, a murine model of defective osteoblastogenesis and low turnover osteopenia. J Bone Miner Res **12:**1772–1779.
21. Weinstein RS, Jilka RL, Parfit AM, Manolagas SC 1997 Effects of androgen deficiency on murine bone remodeling and bone mineral density are mediated via cells of the osteoblastic lineage. Endocrinology **138:**4013–4021.
22. Lecka-Czernik B, Gubrij I, Moerman E, Kajkenova O, Lipschitz DA, Manolagas SC, Jilka RL 1999 Inhibition of Osf2/Cbfa1 expression and terminal osteoblast differentiation by PPARγ2. J Cell Biochem **74:**1–14.
23. Kachigan SK 1986 Statistical Analysis. Radius Press, New York, NY, U.S.A., pp. 182–185.
24. Lander ES, Green P, Abrahamson J, Barlow A, Daly MJ, Lincoln SE, Newburg L 1987 MAPMAKER: An interactive computer package for constructing primary genetic linkage maps of experimental and natural populations. Genomics **1:**174–181.
25. Basten CJ, Weir BS, Zeng Z-B 1998 QTL Cartographer: A Reference Manual and Tutorial for QTL Mapping. Department of Statistics, North Carolina State University, Raleigh NC, U.S.A.
26. Zeng Z-B 1994 Precision mapping of quantitative trait loci. Genetics **136:**1457–1468.
27. Churchill GA, Doerge RW 1994 Empirical threshold values for quantitative trait mapping. Genetics **138:**963–971.
28. Doerge RW, Churchill GA 1996 Permutation tests for multiple loci affecting a quantitative character. Genetics **142:**285–294.
29. Lander ES, Botstein D 1989 Mapping Mendelian factors underlying quantitative traits using RFLP linkage maps. Genetics **121:**185–199. See also Erratum*:* Genetics **136:**705.
30. Dietrich WF, Miller J, Steen R, Merchant MA, Damron-Boles D, Husain Z, Dredge R, Daly MJ, Ingalls KA, O'Connor TJ, Evans CA, DeAngelis MM, Levinson DM, Kruglyak L, Goodman N, Copeland NG, Jenkins NA, Hawkins TL, Stein L, Page DC, Lander ES 1996 A comprehensive genetic map of the mouse genome. Nature **380:**149–152. *See also Erratum:* Nature **381:**172.
31. Lynch M, Walsh B 1998 Genetics and Analysis of Quantitative Traits. Sinauer Associates, Inc., Sunderland, MA, U.S.A.
32. Klein RF, Mitchell SR, Phillips TJ, Belnap JK, Orwoll ES 1998 Quantitative trait loci affecting peak bone mineral density in mice. J Bone Miner Res **13:**1648–1656.

33. Shimizu M, Higuchi K, Bennett B, Xia C, Tsuboyama T, Kasai S, Chiba T, Fujisawa H, Kogishi K, Kitado H, Kimoto M, Takeda N, Matsushita M, Okumura H, Serikawa T, Nakamura T, Johnson TE, Hosokawa M 1999 Identification of peak bone mass QTL in a spontaneously osteoporotic mouse strain. Mamm Genome **10:**81–87.
34. Johnson ML, Gong G, Kimberling W, Recker SM, Kimmel DB, Recker RB 1997 Linkage of a gene causing high bone mass to human chromosome 11 (11q12–13). Am J Hum Genet **60**:1326–1332.
35. Spiegelman BM, Flier JS 1996 Adipogenesis and obesity: Rounding out the big picture. Cell **87:**377–389.
36. Kodama Y, Takeuchi Y, Suzawa M, Fukumoto S, Kurokawa T 1996 Reduced expression of interleukin-11 from bone marrow stromal cells of Senescence-Accelerated Mice (SAMP6): A role for impaired osteoblast and osteoclast formation. J Bone Miner Res 11:s105 (abstract).
37. Abe E, Yamamoto M, Taguchi Y, Lecka-Czernik B, Economides AC, Stahl N, Jilka RL, Manolagas SC 1998 Requirement of BMPs-2/4 for postnatal osteoblast as well as osteoclast formation: Antagonism by noggin. J Bone Miner Res **13:**s242 (abstract).

Address reprint requests to:
Robert J. Shmookler Reis
J. L. McClellan Veterans Medical Center
4300 West Seventh Street, Research-151
Little Rock, Arkansas 72205 U.S.A.

Received in original form June 17, 1999; in revised form November 1, 1999; accepted November 24, 1999.